Modal identification of time-varying systems using Hilbert transform and signal decomposition

M. Bertha[1], **J.-C. Golinval**[1]
[1] University of Liège, Aerospace & Mechanical Engineering Department, LTAS-VIS
Chemin des chevreuils 1, B-4000, Liège, Belgium
e-mail: **mathieu.bertha@ulg.ac.be**

Abstract
The present work investigates modal identification of time-varying dynamical systems by exploiting the Hilbert transform. The proposed method, initially based on the Hilbert Vibration Decomposition (HVD) method, first identifies the instantaneous frequencies of the system. Their corresponding components and modal deflection shapes are then extracted from a set of dynamic responses of the system. The proposed method is first presented and then is illustrated on an experimental set-up. The system under investigation is a recurrent experiment in the field of time-varying systems consisting in a beam travelled by a non-negligible mass while excited by a random external force. The results highlight the time dependency of the modal parameters of the system due to the variant position of the mass with time.

1 Introduction

For several years, modal identification of dynamical systems showing dependencies with respect to time or other parameters has increased in interest. Because of these dependencies, the structural responses are nonstationary and therefore, a large variety of signal processing tools are lost for the identification because they rely on the assumption that the signals are stationary. For this reason, new techniques were used to overcome this nonstationary behaviour. For example, the short-time Fourier transform, the wavelet transform or the Wigner-Ville distribution are good example of tools able to represent a signal in the time and frequency domains simultaneously. Another way to study the nonstationarity in signals is to split them into their constitutive components and to study them separately. One can cite for example the *Hilbert-Huang Transform* (*HHT*) [1], able to decompose nonstationary and nonlinear signals into monocomponents, called *Intrinsic Mode Functions* (*IMF*), having their own time-varying amplitude and frequency. Similarly to the HHT method, a most recent one, the *Hilbert Vibration Decomposition* (*HVD*) [2, 3], is also able to sift vibration signals into their constitutive monocomponents. Finally, one also can cite a variety of time varying autoregressive models able to tracks the signal properties.

The paper is organized as follows. First, the Hilbert transform is introduced and, because the initial work is based on the idea of the Hilbert Vibration Decomposition method, the latter one is also shortly presented. A way to estimate the instantaneous frequencies in a signal through autoregressive modelling is then described and it is shown how it can be introduced in the philosophy of the HVD method, i.e. find the instantaneous frequencies and then decompose the signal into monocomponents. Finally, an experimental set-up is presented and the results of the time-varying identification are discussed.

2 The Hilbert transform and the *Hilbert Vibration Decomposition* method

2.1 The Hilbert transform

The Hilbert transform is a particular linear transformation remaining in the same domain as the signal to be transformed. When applied to an oscillatory signal it results in a new signal in phase quadrature with respect to the original one (phase shift of $-\pi/2$ radian). The Hilbert transform of a signal $x(t)$ can be calculated by its convolution with the function

$$h(t) = \frac{1}{\pi\, t}.$$

Using the phase quadrature property of the transformed signal, it is possible to build an *analytic form* of the original signal by addition of its Hilbert transform multiplied by the complex unit j. The latter analytic signal has the form of a rotating phasor in the complex plane and can be described by its instantaneous phase $\phi(t)$ and amplitude $a(t)$:

$$\begin{aligned} z(t) &= x(t) + j\,\tilde{x}(t) \\ &= a(t)\, e^{j\,\phi(t)}. \end{aligned} \tag{1}$$

Using (1), the amplitude and phase can easily be obtained as the absolute value of the analytic signal, $a(t) = |z(t)|$ for the instantaneous amplitude, and its phase is given by the argument of the complex signal $\phi(t) = \angle z(t)$. The instantaneous frequency is then calculated as the time derivative of the phase angle. An illustration of this transform on a damped sinusoid signal is shown in Figure 1(a).

A useful and important property of the Hilbert transform is the *Bedrosian product theorem* [4] which concerns the transformation of a product of functions. It stipulates that if $u(t)$ and $v(t)$ are two functions characterised by a low and a high (but non overlapping) spectra, respectively, the low frequency signal can be extracted of the transformation s.t. :

$$\mathcal{H}(u(t)\, v(t)) = u(t)\, \mathcal{H}(v(t)). \tag{2}$$

2.2 The Hilbert Vibration Decomposition method

In his book and tutorial [2, 3], Feldman present a method to perform the separation of a signal into its monocomponents based on the Hilbert transform.

2.2.1 The sifting process of the HVD method

Looking at the analytic form of a multicomponent signal, the sum of all individual phasors describe a global rotating trajectory in the complex plane as illustrated in Figure 1(b).

In the complex plane representation of the signal, the followed trajectory is driven by the component having the highest amplitude and the other component add oscillations around this main trajectory. The HVD method focuses on this main trajectory by filtering the lower amplitude components and gets its time varying frequency. This frequency is then used in a synchronous detection step for its monocomponent extraction from the signal.

Given a vibrating signal $x(t)$, the HVD method can be summarized as follows :

1. Compute the analytic signal $z(t)$ from $x(t)$;
2. Get the instantaneous frequency of the analytic signal;
3. Lowpass the instantaneous frequency to filter the contribution of the lower amplitude components;

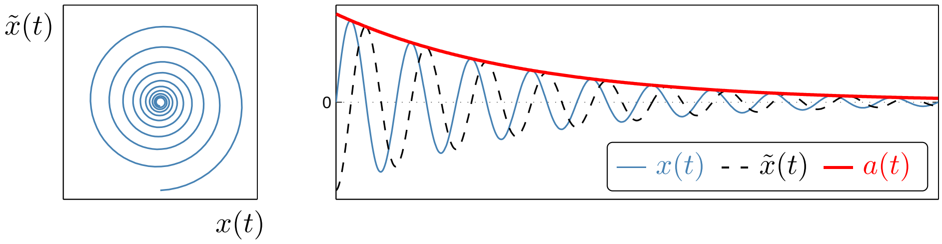

(a) One component damped signal.

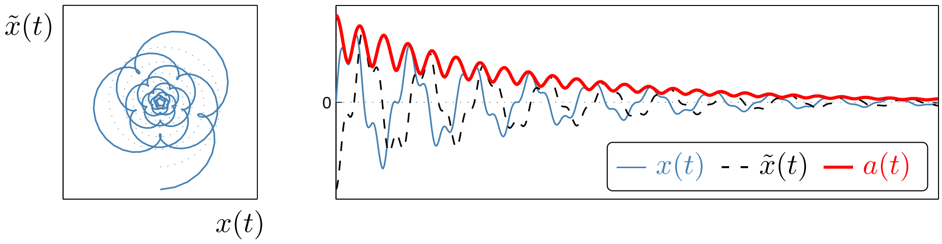

(b) Two-components damped signal.

Figure 1: Signal, Hilbert transform, amplitude and trajectory in the complex plane of a single component (a) and a two-components signal (b).

4. Extract the higher amplitude component by synchronous detection with the previously lowpassed frequency;
5. Extract this component from the signal and iterate until no more components are present in the signal.

However, because the HVD method focuses on the higher amplitude monocomponent, if the amplitude of some constitutive monocomponents in the signal cross themselves, the HVD method will always follow the one with the higher amplitude and then the extracted component may contain parts of different modes at different instants. A way to overcome this drawback is presented in the next section with application to multiple signals.

2.2.2 Application to multi-degree-of-freedom systems

As explained previously, the HVD method may be perturbed by crossings in amplitude between monocomponents. Further, another difficulty appears when trying to study multiple signals at the same time. The idea we proposed in previous papers [5, 6] to overcome this difficulty was to introduce a source separation step into the main algorithm of the HVD method. By performing a source separation, each source mainly gathers the information of one particular mode and decreases the influence of the others. In that way, the estimation of the instantaneous frequency on each source is better and furthermore, we only have one instantaneous frequency curve per mode instead of having one curve in each channel.

Nevertheless, the use of source separation is not a panacea and some limitations may occur when trying to enlarge the studied frequency band. By enlarging the frequency band, higher frequency modes of vibration are introduced and, as it will be shown in Section 4.3, the nonstationary effect increases with the frequency and becomes too significant to be handled by the source separation methods. It is the reason why, in the following, another approach is proposed for the instantaneous frequencies estimation.

3 Alternative approach to the instantaneous frequencies estimation and synchronous detection

3.1 Time-Varying Auto Regressive model for the identification of instantaneous frequencies

Several methods are available for parameters estimation in time-varying processes [7]. We focus here on basis functions based autoregressive models which are also widely used by Poulimenos and Fassois in various formulations [8]. Autoregressive models are based on the representation of an output signal $x(t)$ as a linear combination of its past values

$$x(t) = \sum_{i=1}^{p} a_i \, x(t-i) + e(t) \tag{3}$$

in which the a_i ($i = 1, \ldots, p$) are the regression coefficients to be identified and $e(t)$ represents a stationary white noise.

If the system generating the response is time-dependent, the regression parameters are not constant anymore and also show a time dependency so that the autoregressive model becomes

$$x(t) = \sum_{i=1}^{p} a_i(t) \, x(t-i) + e(t). \tag{4}$$

The time variation of the a_i parameters renders their identification more difficult. The idea behind the basis functions approach is to model the time-varying coefficients as a linear combination of a set of previously selected time functions:

$$a_i(t) = \sum_{k=0}^{q} a_{i,k} \, u_k(t). \tag{5}$$

Introducing the approximation of the regressive coefficients (5) into (4), the problem writes

$$x(t) = \sum_{i=1}^{p} \sum_{k=0}^{q} a_{i,k} \, u_k(t) \, x(t-i) + e(t). \tag{6}$$

where the coefficients $a_{i,k}$ become the parameters to be identified. p and q refer to the model order and the order of the functions basis, respectively. Let us note that this operation transform the initial time-varying problem into a time invariant one because the coefficients $a_{i,k}$ do not depend on time anymore. In the frequency domain, the time-varying autoregressive model (4), is equivalent to a filter characterised by a time-varying transfer function

$$H(\omega, t) = \frac{1}{1 - \sum_{i=1}^{p} a_i(t) \, e^{-j\,\omega\, i}}. \tag{7}$$

Let us now introduce the following vector notations :

- **the regression vector :** $\boldsymbol{\varphi}(t) = [x(t-1),\, x(t-2),\, \ldots,\, x(t-p)]^T$ which gathers the p lagged values of x;
- **the regression coefficients vector :** $\boldsymbol{a}(t) = [a_1(t),\, a_2(t),\, \ldots a_p(t)]^T$ which gathers the time-varying regression coefficients;
- **the basis functions vector :** $\boldsymbol{u}(t) = [u_0(t),\, u_1(t),\, \ldots u_q(t)]^T$ which gathers the $q+1$ basis functions;
- **the generalized regression vector :** $\boldsymbol{\psi}(t) = \boldsymbol{\varphi}(t) \otimes \boldsymbol{u}(t)$, where $\otimes$ denotes the Kronecker product;

- **the generalized regression coefficients vector :** $\boldsymbol{\alpha} = \left[\boldsymbol{\alpha}_1^T,\, \boldsymbol{\alpha}_2^T, \ldots \boldsymbol{\alpha}_p^T\right]^T$, in which $\boldsymbol{\alpha}_i = [a_{i,0},\, a_{i,1},\, \ldots, a_{i,q}]^T$, gathers the time invariant coefficients to be estimated.

With these notations, the time-varying autoregressive coefficients in Equation (4) can now be rewritten into a vector form:

$$\begin{aligned} x(t) &= \sum_{i=1}^{p} a_i(t)\, x(t-i) + e(t) \\ &= \boldsymbol{\varphi}^T(t)\, \boldsymbol{a}(t) + e(t) \\ &= \boldsymbol{\psi}^T(t)\, \boldsymbol{\alpha} + e(t) \end{aligned} \tag{8}$$

The extended set of coefficients in the $\boldsymbol{\alpha}$ vector in (8) may then be estimated using the least squares method:

$$\begin{aligned} \boldsymbol{\alpha} &= \arg\min_{\boldsymbol{\alpha}} \sum_{t=1}^{N} \left(x(t) - \boldsymbol{\psi}^T(t)\, \boldsymbol{\alpha}\right)^2 \\ &= \left(\sum_{t=1}^{N} \boldsymbol{\psi}(t)\, \boldsymbol{\psi}^T(t)\right)^{-1} \left(\sum_{t=1}^{N} x(t)\, \boldsymbol{\psi}(t)\right) \end{aligned} \tag{9}$$

with N the number of useful data points in the time series. Combining the coefficients in $\boldsymbol{\alpha}$ and the basis functions in $\boldsymbol{u}$, the time-varying regression coefficients in $\boldsymbol{a}$ can be recovered. To obtain the instantaneous frequencies we are looking for, we have first to calculate the time-varying poles of the system, which are computed at each time t as the roots of the polynomial formed by the coefficient in $\boldsymbol{a}(t)$ (zeroes of the denominator of the transfer function (7)). Taking the imaginary part of the instantaneous poles leads to the instantaneous frequencies.

Finally, one can note that:

1. Equation (9) is easily extended to complex valued signals, e.g. after Hilbert transformation of real valued signals, by using complex conjugate and Hermitian transposed.

2. If working with complex valued signals, a model order of p will lead to p instantaneous poles instead of $p/2$ if working with real valued signals because the poles will appear in complex conjugated pairs.

3. Because the poles of a dynamic system are global properties, if several measurements are recorded on the system, they should contain the same poles. So, Equation (9) should give the same $\boldsymbol{\alpha}$ vector of coefficients if they are calculated on each channel. If we have several measurements at our disposal, we can turn Equation (9) into an overdetermined system of equations.
   This procedure is similar to the extension from the *Complex Exponential* (*CE*) method to the *Least-Squares Complex Exponential* (*LSCE*) method made in standard modal analysis [9]. Indeed, the CE method computes the modal parameters by fitting an impulse response function (IRF) of the system, it is so a Single-Input Single-Output (SISO) method. By extension, the LSCE method performs a global fitting of a set several IRFs at the same time, it is then a Single-Input Multiple-Outputs (SIMO) method.

3.2 Extraction of monocomponents and modal deflection shapes

The previous section describes how to get the evolution of the poles of the system. It remains now to investigate how the mode shapes of the structure vary with time. To do so, a Vold-Kalman filter [10] is used to extract the monocomponents and their complex amplitude, related to the instantaneous frequencies previously extracted.

The signal model used in the Vold-Kalman filter method relies on the superposition of monocomponents, the latter being composed of an amplitude modulated by an oscillatory function such as

$$x(t) = \sum_i \underbrace{a_i(t)\, e^{j\,\phi_i(t)}}_{x_i(t)} + e(t) \tag{10}$$

in which $a_i(t)$ is the complex amplitude of the i^{th} component $x_i(t)$ and $e(t)$ is the noise in the signal. The phase evolution $\phi_i(t)$ is simply the time integration of the i^{th} instantaneous frequency which, along with the recorded time signals, are the inputs of the problem. The unknowns to be estimated are the complex amplitudes $a_i(t)$. To do so, the Vold-Kalman filter performs a minimisation of two equations. First, the *Data Equation* optimises the closeness between the model and the data

$$x(t) - \sum_i a_i(t)\, e^{j\,\phi_i(t)} = \delta(t). \tag{11}$$

Then, a set of equations, named the *Structural Equations* involving a difference operator of chosen (but small) order, is added to regularize the problem and ensure the smoothness of the solution:

$$\nabla^{r+1} a_i(t) = \varepsilon_i(t). \tag{12}$$

The minimisation is performed simultaneously on $\delta(t)$ and $\varepsilon_i(t)$ to ensure both the closeness to the signal model and the smoothness of the solution.

Performing the extraction of the complex amplitude on a set of signals, a set of vectors gathering the amplitudes of each signal for each monocomponent is obtained. One may note a similarity between the Vold-Kalman model and the modal expansion of the output signals in linear systems

$$\begin{array}{rlll} \text{Vold-Kalman filter:} & \boldsymbol{x}(t) = \sum_i & \boldsymbol{a}_i(t) & e^{j\,\phi_i(t)} \\ & & \updownarrow & \updownarrow \\ \text{Modal expansion:} & \boldsymbol{x}(t) = \sum_i & \boldsymbol{V}_i(t) & \eta_i(t) \end{array} \tag{13}$$

where the $\eta_i(t)$ are the modal coordinates of the expansion which, by definition, are time functions oscillating at the frequency $\omega_i(t)$. The vector of amplitude $\boldsymbol{a}_i(t)$ is then used as an unscaled version of the i^{th} time-varying mode shape $\boldsymbol{V}_i(t)$.

4 Experimental set-up

To test the present identification method, an experimental set-up was built. The design of this set-up is based on a usual problem already used in several researches. One can cite for example the references [11, 12] in which bridge-like structures were used with a travelling mass to make it vary.

4.1 Set-up description

The experimental set-up consist of a 2.1 meter-long aluminium beam carrying a travelling load made of a steel block. The block-to-beam mass ratio is 38.6 %, which is non negligible and causes a dependence of the system modal parameters with respect to the position of the mass. The beam is supported by springs at both ends with negligible rotating stiffness. The experimental set-up is shown in Figure 2.

The system is instrumented with seven accelerometers (five along the beam on the longitudinal axis and one on each support). It is randomly excited by a shaker located at the position of the first sensor on the beam. The excitation and the acquisition of the responses is performed through a LMS Scadas Mobile system [13] and the Test.Lab software [14].

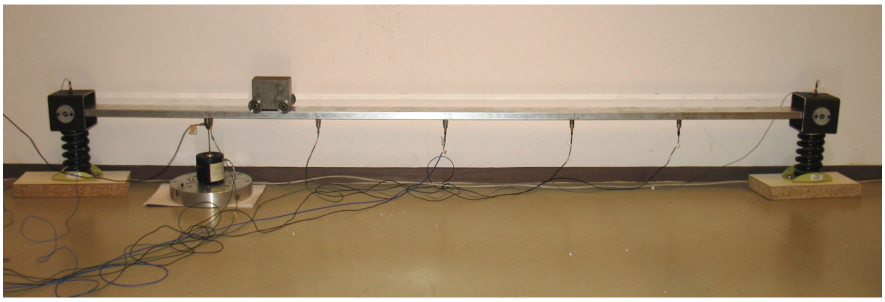

Figure 2: Illustration of the experimental set-up.

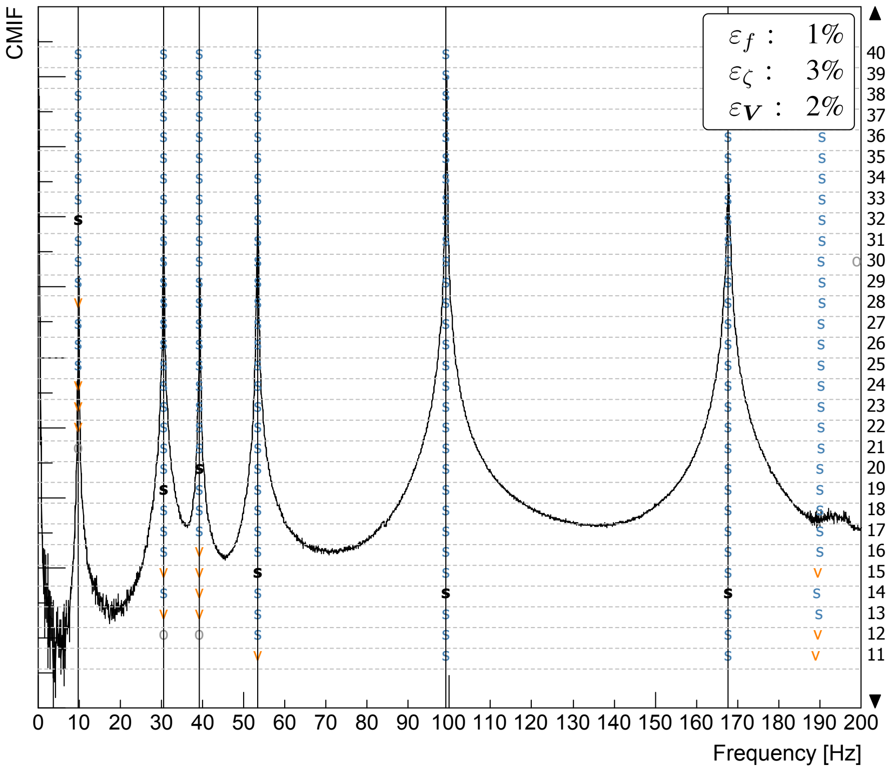

Figure 3: Stabilisation diagram obtained in the modal identification with the PolyMAX method.

4.2 Linear time invariant modal analysis of the system

A first modal identification is performed on the single beam on its supports without the moving mass. The modal analysis is performed in the frequency band of [0, 200] Hz using the PolyMAX method [14] and the corresponding stabilisation diagram is given in Figure 3. The selected stable poles are represented by bold black **s**, leading to the modal parameters listed in Table 1. The results of this identification serve as reference for the comparison with the time-varying modal parameters identified in Section 4.3.

In the frequency band up to 200 Hz, six modes are present and they are characterized by very low damping. Their corresponding mode shapes are represented in Figure 4 in which it can be observed that the shapes of the modes three to six (Figures 4(c) to 4(f)) are very similar to the free-free beam mode shapes.

4.3 Linear time-varying modal analysis

In the following analysis, the steel mass is pulled by hand with a very thin string at approximately constant speed. The travel time is 50 seconds during which the system is randomly excited by the shaker and its

Mode #	Frequency [Hz]	Damping ratio [%]
1	9.79	0.20
2	30.43	0.10
3	39.23	0.20
4	53.32	0.08
5	99.23	0.07
6	167.79	0.16

Table 1: Experimental modal parameters of the supported beam.

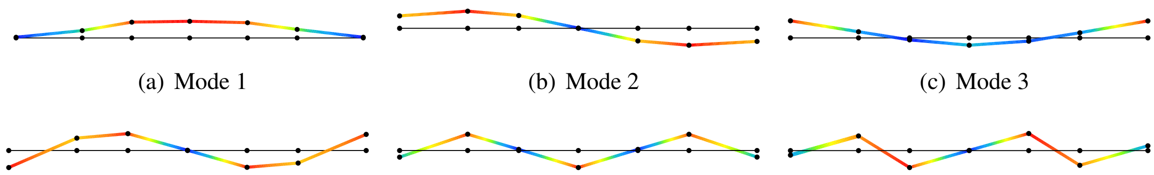

(a) Mode 1 (b) Mode 2 (c) Mode 3

(d) Mode 4 (e) Mode 5 (f) Mode 6

Figure 4: Experimental eigen modes of the structure present in the frequency band [0 200] Hz.

response accelerations at the seven sensors are recorded. The time-frequency dependence of the system is illustrated in Figure 5 using the wavelet transform. It can be seen that the main effect of the motion of the mass is a decrease in frequency at different time instants depending on the mode number. If we assume a constant speed of the mass, the length of the beam can be substituted to the time axis and if we compare with the mode shapes in Figure 4, we see that the decreases are of maximum amplitude when the mass is located at antinodes of vibration. Similarly, the time varying frequencies recover their initial value (black lines on the figure) when the mass passes at nodes of vibration. Another thing to be noticed is that the higher the frequency is, the more significant is the effect of the moving mass.

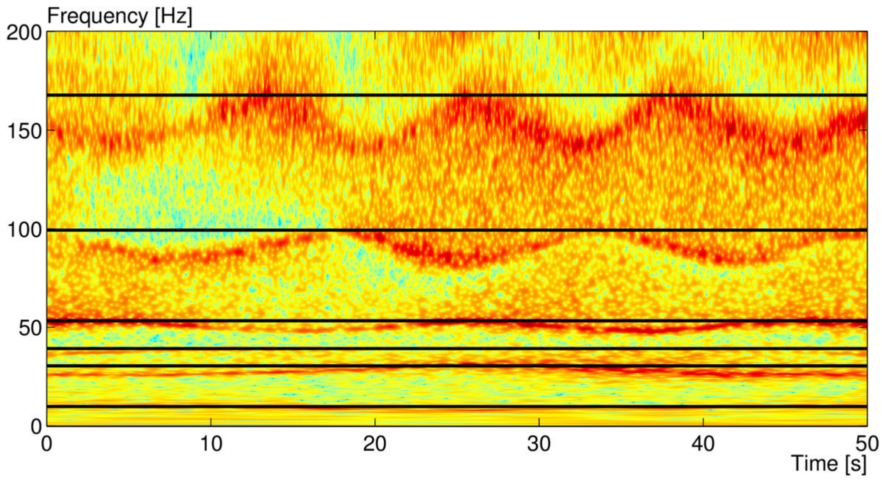

Figure 5: Wavelet transform of the beam at location #3. (The reference frequencies listed in Table 1 are drawn in black lines.)

4.3.1 Instantaneous frequencies estimation

Using the time-varying autoregressive model described in Section 3.1, the poles of the system are now estimated over the recording time span. Applying the TVAR model with a model order of $p = 17$ and a basis

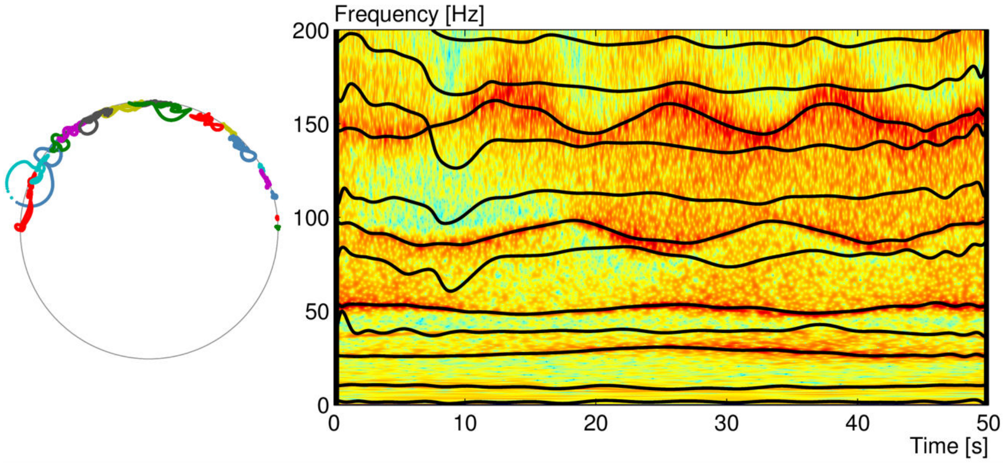

(a) Frequencies related to all poles

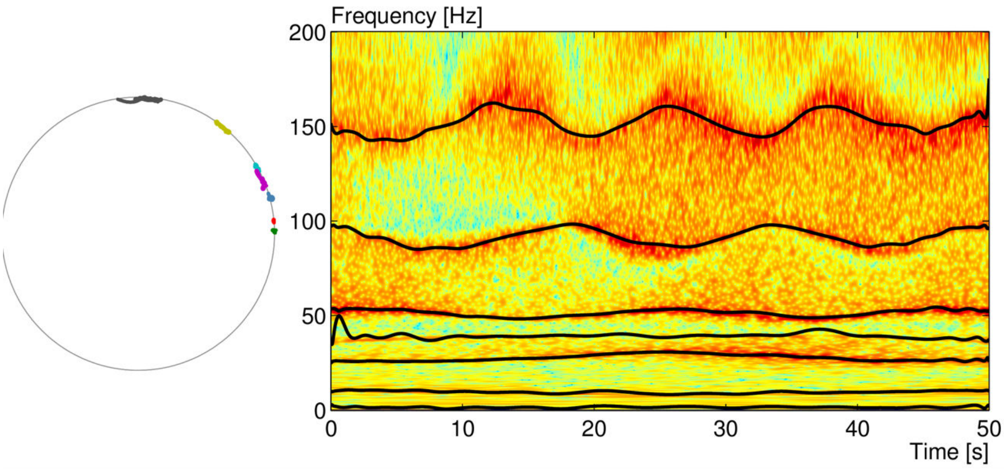

(b) Selected subset of seven poles trajectories

Figure 6: Identified instantaneous frequencies of the system with the complex trajectories of the instantaneous poles.

of $q + 1 = 33$ Legendre polynomials, we get the results depicted in Figure 6(a). On the left hand side of that figure are represented the trajectories of all the estimated poles of the system in the complex plane (17 in this case as the analytic signals are used). But clearly, keeping all the estimated frequencies is not judicious because some of them refer to noise. It is necessary to select the pole trajectories related to physical poles and reject the spurious ones. To do so, Beex and Shan proposed in [15] a simple method which consist in choosing a number m of physical poles to retain and to select the subset of m poles having their trajectory the closest to the unit circle. This is illustrated in Figure 6(b) where seven poles are retained. Seven and not six poles are retained because the trajectory of the lower frequency has a mean radius closer to one than some other physical modes. It will manually be rejected later because of its lack of physical sense.

4.3.2 Decomposition into monocomponents and extraction of modal deflection shapes

Knowing the evolution of the instantaneous frequencies of the system, the last remaining task is to extract their respective monocomponent and their complex amplitude by the Vold-Kalman filter previously described in Section 3.2. As shown in Equation (13), the extracted complex amplitude is considered as a time-varying unscaled version of the mode shapes of the system. Because it is not possible to show the complete evolution of all the mode shapes in this paper, several snapshots along the time axis are considered to be compared

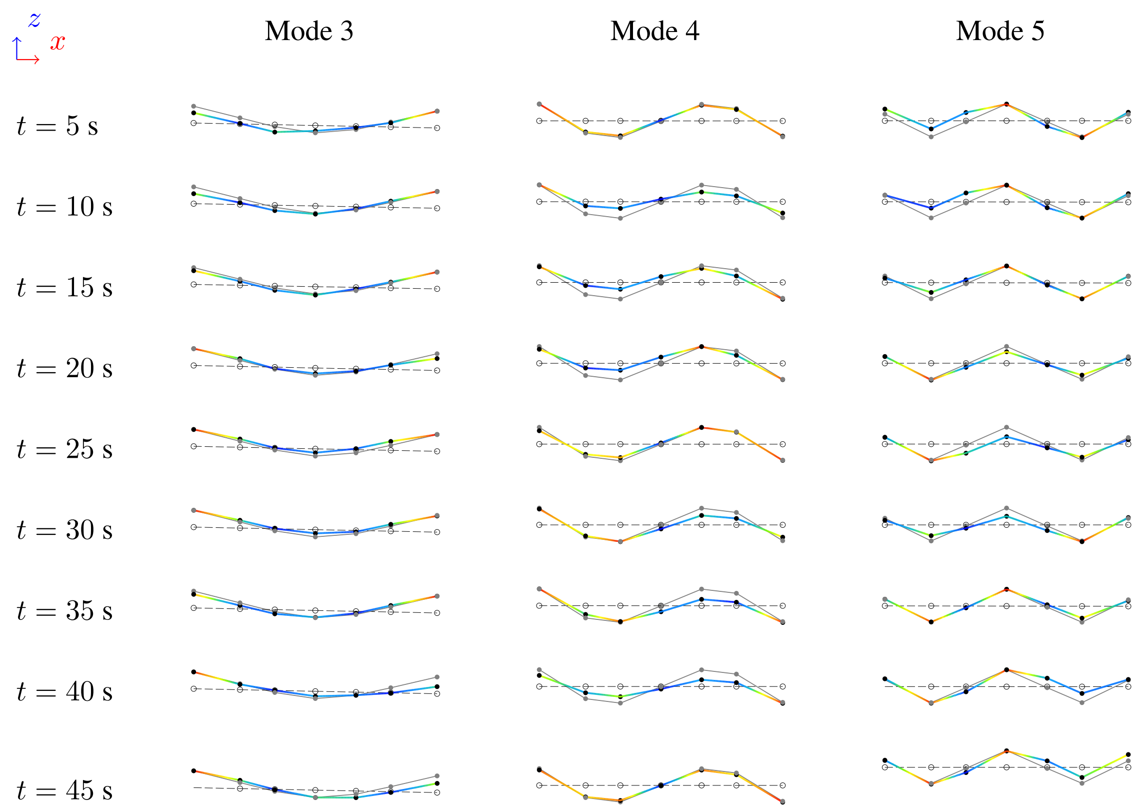

Figure 7: Time evolution of the 3^{rd}, 4^{th} and 5^{th} modes at nine equally spaced snapshots in the recording time. The grey reference deformed shapes are the ones computed in Section 4.2 for the beam-only subsystem (LTI analysis).

with the mode shapes of the time invariant system (Figure 4). Figure 7 shows modes 3, 4 and 5 at several time instants in the total recording time. In the reference frame used to draw these deformed shapes, the mass is initially located on the left hand side and moves to the right with time. Its effect on the dynamics of the system is an addition of inertial forces that give rise to a decrease in amplitude of vibration at its location. This can easily be seen at antinodes of vibration. Further, similarly to what we observed for the instantaneous frequencies, the instantaneous mode shapes are not perturbed anymore when the mass is located at nodes of vibration.

5 Conclusion

This work presented a method for the identification of time-varying dynamic systems. Based on the idea used in the HVD method (i.e. find instantaneous frequencies of the system and demodulate their related monocomponent and amplitude) we introduced a new alternative to the instantaneous frequencies estimation and a way to perform a global analysis using all the outputs at the same time.

The method was tested on a classical experimental system and gave results that are in good agreement with results found in the literature [12]. The dynamics of the time-varying system is well recovered: it shows maximum decreases in frequency and amplitude when the mass passes through antinodes of vibration and conversely, is not perturbed when the mass is located to nodes of vibration.

The next step is now to apply the proposed method on industrial application.

References

[1] N. E. Huang, Z. Shen, S. R. Long, M. C. Wu, H. H. Shih, Q. Zheng, N.-C. Yen, C. C. Tung, and H. H. Liu. *The empirical mode decomposition and the Hilbert spectrum for nonlinear and non-stationary time series analysis*. *Proceedings of the Royal Society A: Mathematical, Physical and Engineering Sciences*, 454(1971):903–995, March 1998.

[2] M. Feldman. *Hilbert Transform Applications in Mechanical Vibration*. John Wiley & Sons, Ltd, Chichester, UK, March 2011.

[3] M. Feldman. *Hilbert transform in vibration analysis*. *Mechanical Systems and Signal Processing*, 25(3):735–802, April 2011.

[4] E. Bedrosian. *A product theorem for Hilbert transforms*. *Proceedings of the IEEE*, 51(5):868–869, 1963.

[5] M. Bertha and J.-C. Golinval. *Identification of a Time-Varying Beam Using Hilbert Vibration Decomposition*. In *Proceedings of IMAC XXXII*, Orlando, 2014.

[6] M. Bertha and J.-C. Golinval. *Experimental modal analysis of a beam travelled by a moving mass using Hilbert Vibration Decomposition*. In *Proceedings of Eurodyn IX*, Porto, 2014.

[7] Maciej Niedzwiecki. *Identification of Time-Varying Processes*. John Wiley & Sons, Inc., New York, NY, USA, 2000.

[8] A.G. Poulimenos and S.D. Fassois. *Parametric time-domain methods for non-stationary random vibration modelling and analysis A critical survey and comparison*. *Mechanical Systems and Signal Processing*, 20(4):763–816, May 2006.

[9] N.M.M. Maia and J.M.M. Silva. *Theoretical and Experimental Modal Analysis*. Research Studies Press Limited, 1997.

[10] C. Feldbauer and R. Höldrich. *Realization of a Vold-Kalman Tracking Filter - A Least Squares Problem*. In *Proceedings of the COST G-6 Conference on Digital Audio Effects (DAFX-00)*, number 8, pages 8–11, Verona, Italy, 2000.

[11] A.G. Poulimenos and S.D. Fassois. *Output-only stochastic identification of a time-varying structure via functional series TARMA models*. *Mechanical Systems and Signal Processing*, 23(4):1180–1204, May 2009.

[12] S. Marchesiello, S. Bedaoui, L. Garibaldi, and P. Argoul. *Time-dependent identification of a bridge-like structure with crossing loads*. *Mechanical Systems and Signal Processing*, 23(6):2019–2028, August 2009.

[13] *LMS SCADAS Mobile*. http://www.lmsintl.com/scadas-mobile.

[14] *LMS Test.Lab*. http://www.lmsintl.com/testlab.

[15] A.A. Beex and P. Shan. *A time-varying Prony method for instantaneous frequency estimation at low SNR*. In *Proceedings of the 1999 IEEE International Symposium on*, pages 5–8, 1999.